

# Fabrication and Characterization of Bimodal Size Al<sub>2</sub>O<sub>3p</sub> Reinforced 7075 Aluminium Matrix Composites

Ruirui WU, Qiushu LI\*, Lu GUO, Yanxiang MA

Taiyuan University of Science and Technology, Taiyuan 030024, Shanxi, China

crossref <http://dx.doi.org/10.5755/j01.ms.23.4.16956>

Received 26 November 2016; accepted 13 April 2017

Bimodal sized (Nano and Micron) Al<sub>2</sub>O<sub>3</sub> particle-reinforced 7075Al matrix composites were prepared by a new method called rotary stirring-injection process. The Al<sub>2</sub>O<sub>3</sub> particles were injected into the molten 7075 alloy through the flows of inert argon gas, and the rotary stirring was used simultaneously. The effect of bimodal sized Al<sub>2</sub>O<sub>3</sub> particles reinforcement with average size of 30–100 nm, 3–5 μm and volume fraction of 1 %, 4 % on microstructure, hardness and tribological properties of 7075 Al-based composite was investigated. Experimental results exhibited fine grains, well-dispersed bimodal sized Al<sub>2</sub>O<sub>3</sub> particles and well-bonded interface between Al<sub>2</sub>O<sub>3</sub> particles and 7075Al matrix. The hardness and wear behavior of the bimodal sized Al<sub>2</sub>O<sub>3p</sub>/7075 composites were significantly enhanced, being compared to the 7075Al matrix and the single sized Al<sub>2</sub>O<sub>3p</sub>/7075 composites.

*Keywords:* composite materials, bimodal sized particles, 7075 alloy, microstructure.

## 1. INTRODUCTION

Particle-reinforced aluminum metal matrix composites (AMMCs), which exhibit high strength, high hardness, good wear resistance and light weight, are widely used in the aerospace, architectural, marine and mineral processing industries [1–3]. It is well known that the particle size has significant influence on the mechanical properties of aluminum metal matrix composites [4, 5]. In general, the micron-sized particles are used to improve the strength of the metal-matrix, while the ductility decreases severely. On the other hand, the nano-sized particles can obviously strengthen the metal-matrix without sacrificing the ductility. However, the agglomerations appear when the content of nano-particles is higher than 1 vol % [6, 7]. This is due to the increasing surface area and surface energy of nano-particles, which cause an increasing tendency for agglomerations of reinforcement particles. Therefore, the mixture of micron-sized and a little amount of nano-sized particles might have significant influence on the mechanical properties of the composites [8, 9].

There are several fabrication techniques to manufacture particle reinforced Al alloy composites. The fabrication methods can be divided into three types. These are solid phase, liquid phase and semi-solid fabrication processes [10]. Many investigators have focused on the commercially important system, liquid process due to its simplicity is more considered. However, the reinforced particles are not readily wetted by liquid Al that can be the most crucial factor in such techniques [11]. So various methods are appeared to improve the wettability of particles in the melt of Al such as: addition of some alloying elements to the melt [12], making a wrapper on the surface of particles by CVD or PVD methods [13],

applying force to the melt and controlling atmosphere [14, 15].

In this paper, a novel rotary stirring-injection process was used to fabricate the bimodal sized (nano and micro) Al<sub>2</sub>O<sub>3p</sub>/7075 composites, which can improve the incorporation of Al<sub>2</sub>O<sub>3p</sub> and 7075 Al matrix. The microstructure, hardness and tribological properties were investigated and the strengthening mechanisms were discussed. This provides a new design idea and methods for the future research.

## 2. EXPERIMENTAL APPARATUS AND PROCEDURE

The bimodal sized Al<sub>2</sub>O<sub>3p</sub>/7075 composites contain 1 vol % of nano-Al<sub>2</sub>O<sub>3p</sub> and 4 vol % of micron-Al<sub>2</sub>O<sub>3p</sub> (denote as “n1 + m4”). To identify the effect of bimodal sized Al<sub>2</sub>O<sub>3p</sub> on the 7075 Al matrix, nano 1 vol % (denote as “n1”) and micron 4 vol % (denote as “m4”) Al<sub>2</sub>O<sub>3p</sub>/7075 composites were separately fabricated using the same process. Table 1 shows the chemical composition of 7075 alloy, this alloy was used as matrix in the experiment, also Al<sub>2</sub>O<sub>3</sub> particles (selected as the reinforcement) with the diameter of 30–100nm and 3–5 μm were prepared.

**Table 1.** The chemical composition of 7075 alloy

Zn	Mg	Cu	Mn	Ti	Gr	Si	Fe	Al
5.23	2.1	1.45	0.3	0.16	0.23	0.22	0.22	-

Fig. 1 shows the schematic of designed equipment that was used in this paper. The preparation process was described as follows: Initially, a certain amount of 7075 Al was charged into the graphite crucible and heated up to 700 °C for completely melting. Then the stirring and injection process were applied. The stirrer was preheated before immersing in the melt and located approximately at the depth of 2/3 height of the molten metal in the crucible. The argon gas flowed through the center of hollow stirring rod, after stirring for 5 minutes the mixed Al<sub>2</sub>O<sub>3</sub> particles

\* Corresponding author. Tel.: +8613994250965.  
E-mail address: [lqslsdyx@126.com](mailto:lqslsdyx@126.com) (Q.S. Li)

were fed into the molten matrix along with the flowing gas. The rotary stirring and injection process continued for about 20 minutes to make the reinforcement particles into the melt. Finally, the molten metal was heated to 720°C immediately and pored into the sand mold.

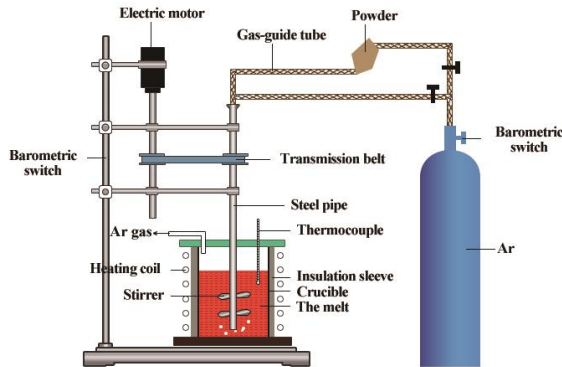


**Fig. 1.** Schematic sketch of experimental setup

The phase compositions of the sample materials were characterized by using X-ray diffraction (XRD; X'PertPRO, D/MAX-2500). The Cu-K $\alpha$  line generated at 40 kV and 200 mA was carried out to identify the phases of the investigated alloys. For microstructure study, the composites and matrix alloy were carried out by optical microscopy (OM;VHX-600) and transmission electron microscope (TEM;JEM-2100F). The OM specimens were prepared according to the standard procedures, grinded through 200, 400, 600, 1000, and 1500 grit papers and etched with a solution (HF (2 ml), HCl (3 ml), HNO<sub>3</sub> (5 ml) and distilled water (190 ml)) for 15 s. The TEM specimens, 0.5 mm in thickness, were cut by spark erosion and slowly thinned to 30  $\mu$ m in thickness by 600 and 2000 grit abrasive papers, followed by punching 3 mm diameter discs. Finally, the discs were ion beam thinned. The Brinell hardness tests were carried out under a HBS-62.5 tester with a ball of 1.0 mm diameter at a load of 10 kg. Dry sliding wear tests were carried out by using a CFT-1 type pin-on-disk machine. The cast sample was the disk (30 mm diameter and 10 mm height) and the pin was steel with a hardness of 62 HRC. The applied load reached 25 N with sliding speed of 600 r/min and the radius to 5 mm for 15 minutes at the room temperature.

### 3. RESULTS AND DISCUSSION

XRD investigations were carried out to identify the phases presented in the composite samples with various Al<sub>2</sub>O<sub>3</sub> particles, and the results were illustrated in Fig. 2, It

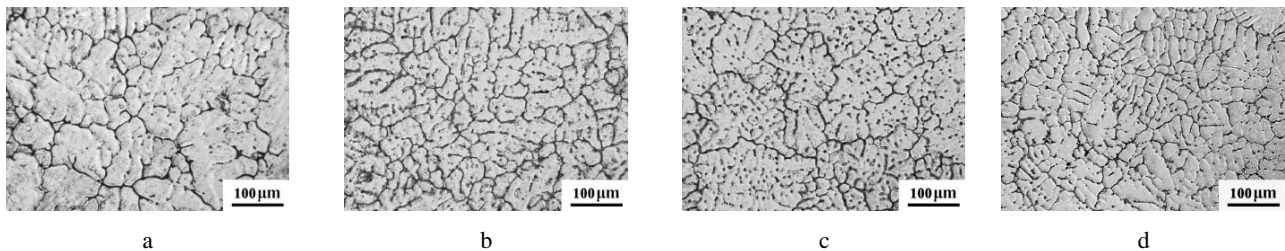


**Fig. 3.** The OM micrographs: a–of as-cast 7075 alloy; b–n1-Al<sub>2</sub>O<sub>3</sub>p/7075Al; c–m4-Al<sub>2</sub>O<sub>3</sub>p/7075Al; d–(n1+m4)-Al<sub>2</sub>O<sub>3</sub>p/7075Al composites

could be seen that diffraction peaks associated with the Al phase and the Al<sub>2</sub>O<sub>3</sub> phase were presented in the as-cast Al<sub>2</sub>O<sub>3</sub>p/7075 composites samples. As seen from Fig. 2 b and d), the intensity of Al<sub>2</sub>O<sub>3</sub> peaks increased with the content of Al<sub>2</sub>O<sub>3</sub>p, and this indicated that the Al<sub>2</sub>O<sub>3</sub>p entered into the 7075 Al matrix.

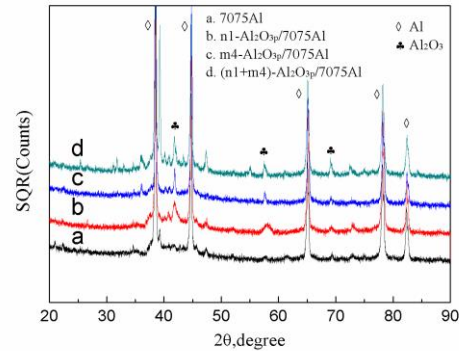


**Fig. 2.** XRD patterns of 7075 Al and Al<sub>2</sub>O<sub>3</sub>p/7075 composites

Fig. 3 shows the optical micrographs of the as-cast 7075 Al and the composites with various Al<sub>2</sub>O<sub>3</sub> particles. As indicated, in the as-cast 7075 Al (Fig. 3 a), the average size of 7075 Al grains is 107  $\mu$ m. In the n1-Al<sub>2</sub>O<sub>3</sub>p/7075 composites, the average size of 7075 grains is 77  $\mu$ m (Fig. 3 b). This is because the Al dendrites solidify firstly during solidification, and the Al<sub>2</sub>O<sub>3</sub> particles act as nucleation sites during the solidification process [16], or act as barriers to dislocations. In the m4-Al<sub>2</sub>O<sub>3</sub>p/7075 composites, the grain size is little different from that of the 7075 alloy (Fig. 3 c), and it appears some black points in the microstructure. Furthermore, the average size of  $\alpha$ -Al grains in the (n1 + m4)-Al<sub>2</sub>O<sub>3</sub>p/7075 composites is smaller than others as shown in Fig. 3 d. It can be observed that the bimodal sized particles have a significant effect on refining the grain size of as-cast composites, which are also shown in the previous studies [17, 18].

In order to study the effects of the rotary stirring-injection process on distribution of the reinforcement particles in the cast composite samples, a quantitatively analysis was applied. At first, specimens from bottom, middle and top piece of each composite sample were prepared and then pictures from different parts of each specimen were taken. Subsequently, different Al<sub>2</sub>O<sub>3</sub> particles werw calculated using the image analyzer and the average volume percentage (AVP) for each sample was reported according to Eq. 1:

$$AVP = \frac{\sum_{i=1}^n \text{volume.percent.}i}{n}, (n=10-20). \quad (1)$$

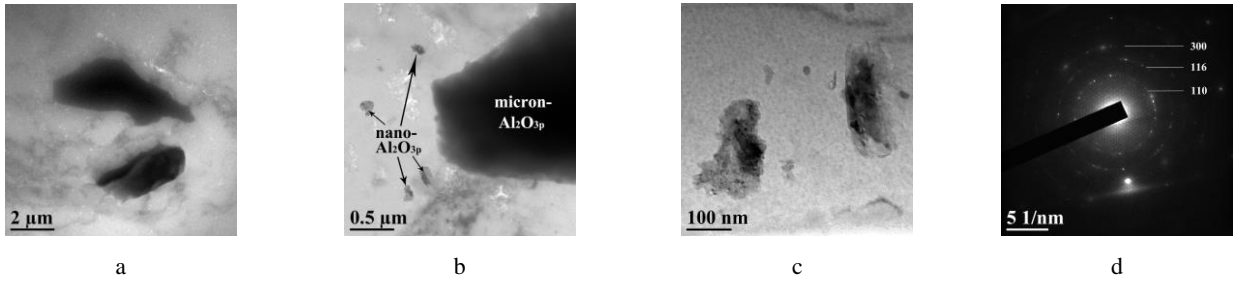


**Fig. 4.** a—the TEM micrographs of (n1+m4)-Al<sub>2</sub>O<sub>3p</sub>/7075Al composites; b—the micron-Al<sub>2</sub>O<sub>3p</sub> boundary and distribution of nano-Al<sub>2</sub>O<sub>3p</sub>; c, d—shows the nano-Al<sub>2</sub>O<sub>3p</sub> and electron diffraction pattern

The results of image analyzing are listed in Table 2. Distribution factor (*DF*) has been defined as the difference between the volume percentages of dispersed particles in the different part of samples and calculated according to:

$$DF(\%) = 100 - \frac{|\max(\min)VP - AVP| \times 100}{AVP}, \quad (2)$$

where  $\max(\min) VP$  is the maximum(minimum) volume percentage for the sample; *AVP* is the average volume percentage (*AVP*) for each sample.

**Table 2.** Volume percent and distribution of Al<sub>2</sub>O<sub>3p</sub> on the surface of samples

Sample	Average volume percent of particles ( <i>AVP</i> )	Distribution factor ( <i>DF</i> )
n1-Al <sub>2</sub> O <sub>3p</sub> /7075Al	0.36	53
m4-Al <sub>2</sub> O <sub>3p</sub> /7075Al	2.23	78
(n1 + m4)Al <sub>2</sub> O <sub>3p</sub> /7075Al	2.85	70

As it can be seen, the rotary stirring-injection process has the ability to fabricate composites with homogenous distribution of reinforcement particles and the method has the most effect on the uniform distribution of particles.

Fig. 4 shows the TEM microstructures of the (n1+m4)-Al<sub>2</sub>O<sub>3p</sub>/7075 composites. By the observation of Al<sub>2</sub>O<sub>3p</sub> in Fig. 4 a, it can be seen that the distribution of micron-Al<sub>2</sub>O<sub>3p</sub> in the 7075Al matrix is uniform. Fig. 4 b shows the higher magnification of Fig. 4 a, which illustrates that the micron-Al<sub>2</sub>O<sub>3p</sub> bonded well with the matrix, and many nano-Al<sub>2</sub>O<sub>3p</sub> were distributed around the micron-Al<sub>2</sub>O<sub>3p</sub>. The nano-Al<sub>2</sub>O<sub>3p</sub> were also bonded well with the 7075 alloy (Fig. 4 c), and the interface between Al<sub>2</sub>O<sub>3p</sub> and 7075 Al matrix is clean. Fig. 4 d shows the electron diffraction pattern of nano-Al<sub>2</sub>O<sub>3p</sub>, and demonstrates that the nano-Al<sub>2</sub>O<sub>3p</sub> are consistent with a hexagonal lattice cubic structure. The results showed that Al<sub>2</sub>O<sub>3p</sub> successful incorporate into 7075Al matrix. Fig. 5 gives the hardness bar graph of the as-cast 7075 alloy and Al<sub>2</sub>O<sub>3p</sub>/7075 composites. It can be seen that under a HBS-62.5 tester with a ball of 1.0 mm diameter at a load of 10 kg, the hardness of the (n1 + m4)Al<sub>2</sub>O<sub>3p</sub>/7075 composites were higher than that of the non-reinforced alloy and single-sized Al<sub>2</sub>O<sub>3p</sub> reinforced composites. The hardness of the (n1 + m4)Al<sub>2</sub>O<sub>3p</sub>/7075 composites are remarkably improved from HB 76 to HB 126 comparing with the as-cast 7075 alloy. Besides, in contrast to the

(n1 + m4)Al<sub>2</sub>O<sub>3p</sub> /7075 composites, the addition of n1-Al<sub>2</sub>O<sub>3p</sub> and m4-Al<sub>2</sub>O<sub>3p</sub> obviously enhances from HB 109 and HB 113 to HB 126.

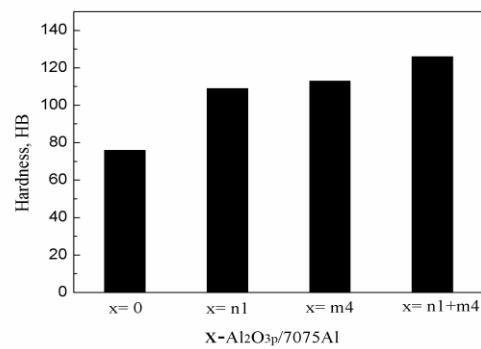


**Fig. 5.** Hardness of 7075 alloy and Al<sub>2</sub>O<sub>3p</sub>/7075 composites

Fig. 6 shows SEM morphologies of the worn surfaces of as-cast 7075 alloy and Al<sub>2</sub>O<sub>3p</sub>/7075 composites generated at the normal load of 25 N, sliding velocity of 600 r/min, the radius is 5 mm, and sliding time of 15 min. In the same wear conditions, the smaller wear width and wear volume, the better wear resistance of the material.

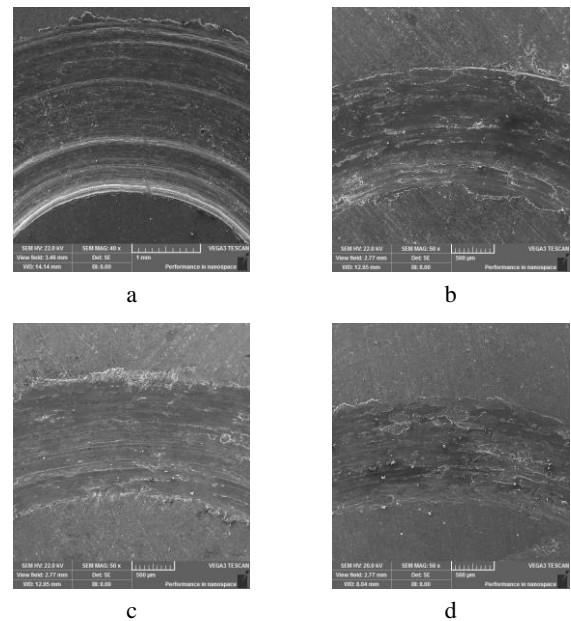


**Fig. 6.** SEM morphologies of the worn surface: a—of as-cast 7075 alloy; b—n1; c—m4; d—n1+m4 Al<sub>2</sub>O<sub>3p</sub>/7075 composites

**Table 3.** The hardness and tribological properties of the composites

Sample	Hardness, HB	Tribological properties		
		Groove width, mm	Groove depth, $\mu\text{m}$	Wear lose, $\text{mm}^3$
7075Al	76	1.726	148.67	0.6755
n1-Al <sub>2</sub> O <sub>3p</sub> /7075Al	109	1.524	118.07	0.4686
m4-Al <sub>2</sub> O <sub>3p</sub> /7075Al	113	1.472	114.51	0.4382
(n1+m4)Al <sub>2</sub> O <sub>3p</sub> /7075Al	126	1.383	87.97	0.3318

Compared a-d, as it can be seen the wear scar width of the (n1 + m4)-Al<sub>2</sub>O<sub>3</sub>/7075 composites is smaller than others. During dry sliding, it seems that the Al<sub>2</sub>O<sub>3p</sub> do not easily come out in debris, which might verify good bonding between Al<sub>2</sub>O<sub>3</sub> particles and the matrix. The nano-Al<sub>2</sub>O<sub>3p</sub> can act as barriers to dislocations and the micro-Al<sub>2</sub>O<sub>3p</sub> can act as load supporting elements. Also according to Archard equation, due to higher hardness of composite sample, the wear resistance of Al<sub>2</sub>O<sub>3</sub>/7075 composites are better than 7075 alloy. Table 3 gives the hardness and tribological properties of the as-cast 7075 alloy and Al<sub>2</sub>O<sub>3p</sub>/7075 composites. It can be seen that the hardness of the (n1 + m4)Al<sub>2</sub>O<sub>3p</sub>/7075 composites was higher than that of the non-reinforced alloy and single-sized Al<sub>2</sub>O<sub>3p</sub> reinforced composites. The groove width, depth and wear lose were smallest. During dry sliding, the Al<sub>2</sub>O<sub>3p</sub> did not easily come out from 7075 matrix, which might show good bonding between Al<sub>2</sub>O<sub>3</sub> particles and the matrix.

The change of mechanical properties mainly depends on the following reasons according to this experiment:

1. Strengthening from grain refinement: In this system, the 7075 matrix grain changed (Fig. 3) after Al<sub>2</sub>O<sub>3p</sub> being added and thereby its mechanical properties excessively changed. The rotary stirring-injection process also have influence on the grain size. Firstly, stirring process causes to break the dendrite shaped structure and leave the structure in small form [19]. Secondly, the Al<sub>2</sub>O<sub>3p</sub> were injected into the molten metal with argon gas, then the particles would be moving along with the stirring molten metal and argon gas, and this would facilitate the incorporation between Al<sub>2</sub>O<sub>3p</sub> and the 7075 matrix. With the stirring and injection process, it can be sure that the Al<sub>2</sub>O<sub>3p</sub> entered into 7075 alloy matrix (Fig. 2), distributed uniform, bonded well, and the interface between Al<sub>2</sub>O<sub>3p</sub> and 7075 Al matrix is clean (Fig. 4). So the improvement of mechanical properties can be explained by A general relationship between micro hardness and grain size proposed by Hall-Petch according to  $H_v = H_{v0} + KD^{-1/2}$  equation ( $H_v$ ,  $H_{v0}$ ,  $K$  and  $D$  are micro hardness, constant, locking parameter and grain diameter, respectively) [20].
2. Strengthening from reinforced particles size: The micron-Al<sub>2</sub>O<sub>3p</sub> can act as load supporting elements in the 7075 matrix, especially used to strengthen the wear resistance. The interaction of dislocations from the nano-Al<sub>2</sub>O<sub>3p</sub> can increase the strength of composite samples according to the Orowan mechanism in this system. The bimodal Al<sub>2</sub>O<sub>3p</sub> as fine particles throughout the matrix can act as barriers to dislocations and load supporting elements, and the well bonded interfaces between bimodal sized Al<sub>2</sub>O<sub>3p</sub> and 7075 matrix can benefit for the effective transfer

of load from the matrix to the particles, So that the mechanical properties were elevated.

#### 4. CONCLUSIONS

The Bimodal sized Al<sub>2</sub>O<sub>3p</sub>/7075 alloy composites were successfully fabricated by the rotary stirring-injection method. The process included mixture of bimodal Al<sub>2</sub>O<sub>3</sub> particles, injection of mixed particles within the melt 7075 aluminum alloy by inert argon gas and stirring the melt. The particles would be moving along with the stirring molten metal and argon gas, and this would facilitate the incorporation between Al<sub>2</sub>O<sub>3p</sub> and the 7075 matrix. The stirring process also causes to break the dendrite shaped structure and leave the structure in small form. This study shows that the bimodal sized Al<sub>2</sub>O<sub>3p</sub>/7075 composites exhibited fine grains, homogeneous bimodal sized Al<sub>2</sub>O<sub>3</sub> particles distribution and well-bonded interface between Al<sub>2</sub>O<sub>3</sub> particles and 7075 Al matrix. The hardness and wear behavior of the bimodal sized Al<sub>2</sub>O<sub>3p</sub>/7075 composites were significantly enhanced, being compared to the 7075 Al matrix and the single sized Al<sub>2</sub>O<sub>3p</sub>/7075 composites. The improvements may be attributed to grain refinement, uniform bimodal sized Al<sub>2</sub>O<sub>3p</sub> distribution and load transfer effect strengthening.

#### Acknowledgments

This work was supported by “Jincheng Science and Technology Project in Shanxi” (China)(No.201501004-13) and “Graduate Student Education Innovation Project in Shanxi” (China)(2016BY137).

#### REFERENCES

1. Tahamtan, S., Halvae, A., Emamy, M., Zabih, M.S. Fabrication of Al/A206-Al<sub>2</sub>O<sub>3</sub> Nano/Micro Composite by Combining Ball Milling and Stir Casting Technology *Materials and Design* 49 2013: pp. 347–359.
2. Li, W.J., Deng, K.K., Zhang, X., Wang, C.J., Kang, J.W., Nie, K.B., Liang, W. Microstructures, Tensile Properties and Work Hardening Behavior of Sicp/Mg-Zn-Ca Composites *Journal of Alloys and Compounds* 695 2017: pp. 2215–2223. <https://doi.org/10.1016/j.jallcom.2016.11.070>
3. Shanbhag, V.V., Yalamoori, N.N., Karthikeyan, S. Fabrication, Surface Morphology and Corrosion Investigation of Al 7075-Al<sub>2</sub>O<sub>3</sub> Matrix Composite in Sea Water and Industrial Environment *Procedia Engineering* 97 2014: pp. 607–613.
4. Uematsu, Y., Tokaji, K., Kawamura, M. Fatigue Behaviour of Sic-Particulate- Reinforced Aluminium Alloy Composites with Different Particle Sizes at Elevated Temperatures *Composites Science and Technology* 68 2008: pp. 2785–2791.

5. **Wu, C.D., Ma, K.K., Wu, J.L., Fang, P., Luo, G.Q., Chen, F., Shen, Q., Zhang, L.M., Schoenung, J.M., Lavernia, E.J.** Influence of Particle Size and Spatial Distribution of B<sub>4</sub>C Reinforcement on the Microstructure and Mechanical Behavior of Precipitation Strengthened Al Alloy Matrix Composites *Materials Science & Engineering A* 675 2016: pp. 421–430.
6. **Su, H., Gao, W.L., Feng, Z.H., Lu, Z.** Processing, Microstructure and Tensile Properties of Nano-Sized Al<sub>2</sub>O<sub>3</sub> Particle Reinforced Aluminum Matrix Composites *Materials and Design* 36 2012: pp. 590–596. <https://doi.org/10.1016/j.matdes.2011.11.064>
7. **Deng, K.K., Wang, C.J., Wang, X.J.** Microstructure and Strengthening Mechanism of Bimodal Size Particlereinforced Magnesium Matrix Composite *Composites Part A* 43 2012: pp. 1280–1284.
8. **Zhang, L.J., Qiu, F., Wang, J.G., Wang, H.Y., Jiang, Q.C.** Microstructures and Mechanical Properties of the Al2014 Composites Reinforced with Bimodal Sized Sic Particles *Materials Science & Engineering A* 637 2015: pp. 70–74.
9. **Chakravartula, K.N., Rajamalla, N.R.** Two Body Abrasive Wear of Al-Mg-Si Hybrid Composites: Effect of Load and Sliding Distance *Materials Science* 22 (4) 2016: pp. 491–494.
10. **Olszo´wka-Myalska, A., Szala, J., leziona, J., Formanek, B., Myalski, J.** Influence of Al-Al<sub>2</sub>O<sub>3</sub> Composite Powder on the Matrix Microstructure in Composite Casts *Materials Characterization* 49 2003: pp. 165–169.
11. **Sangghaleh, A., Halali, M.** An investigation on the Wetting of Polycrystalline Alumina by Aluminium *Journal of Materials Processing Technology* 197 2008: pp. 156–160.
12. **Hoseini, M., Meratian, M.** Fabrication of in Situ Aluminum–Alumina Composite with Glass Powder *Journal of Alloys and Compounds* 471 2009: pp. 378–382.
13. **Yu, Z., Wu, G., Sun, D., Jiang, L.** Coating of Y<sub>2</sub>O<sub>3</sub> Additive on Al<sub>2</sub>O<sub>3</sub> Powder and its Effect on the Wetting Behaviour in the System Al<sub>2</sub>O<sub>3</sub>/Al *Material Letters* 57 2003: pp. 3111–3116. [https://doi.org/10.1016/S0167-577X\(03\)00006-5](https://doi.org/10.1016/S0167-577X(03)00006-5)
14. **Naji, H., Zebarjad, S.M., Sajjadi, S.A.** The Effects of Volume Percent and Aspect Ratio of Carbon Fiber on Fracture Toughness of Reinforced Aluminum Matrix Composites *Materials Science & Engineering A* 486 2008: pp. 413–420.
15. **Wang, S., Zhu, S.Y., Cheng, J., Qiao, Z.H., Yang, J., Liu, W.M.** Microstructural, Mechanical and Tribological Properties of Al Matrix Composites Reinforced with Cu Coated Ti<sub>3</sub>AlC<sub>2</sub> *Journal of Alloys and Compounds* 690 2017: pp. 612–620. <https://doi.org/10.1016/j.jallcom.2016.08.175>
16. **Mazahery, A., Shabani, M.O.** Characterization of cast A356 alloy reinforced with nano SiC composites *Transactions of Nonferrous Metals Society of China* 22(2) 2012: pp. 275–280. [https://doi.org/10.1016/S1003-6326\(11\)61171-0](https://doi.org/10.1016/S1003-6326(11)61171-0)
17. **Tabandeh Khorshid, M., Jenabali Jahromi, S.A.** Mechanical Properties of Tri-Modal Al Matrix Composites Reinforced by Nano- and Submicron-Sized Al<sub>2</sub>O<sub>3</sub> Particulates Developed by Wet Attrition Milling and Hot Extrusion *Materials and Design* 31 2010: pp. 3880–3884.
18. **Shen, M.J., Wang, X.J., Zhang, M.F., Hu, X.S., Zheng, M.Y., Wu, K.** Fabrication of Bimodal Size Sipc Reinforced AZ31B Magnesium Matrix Composites *Materials Science & Engineering A* 601 2014: pp. 58–64. <https://doi.org/10.1016/j.msea.2014.02.035>
19. **Sajjadi, S.A., Ezatpour, H.R., Beygi, H.** Microstructure and Mechanical Properties of Al-Al<sub>2</sub>O<sub>3</sub> Micro and Nano Composites Fabricated by Stir Casting *Materials Science and Engineering: A* 528 (29–30) 2011: pp. 8765–8771.
20. **Mohsen, H.Z., Mirzaee, O., Saidi, P.** Structural and Mechanical Characterization of Al-Based Composite Reinforced with Heat Treated Al<sub>2</sub>O<sub>3</sub> Particles *Materials and Design* 54 2014: pp. 245–250. <https://doi.org/10.1016/j.matdes.2013.08.036>